Tailoring the FeRh magnetostructural response with Au diffusion

AIP | Journal of Applied Physics

Tailoring the FeRh magnetostructural response with Au diffusion

M. Loving, M. A. de Vries, F. Jimenez-Villacorta, C. Le Graët, X. Liu et al.

Citation: J. Appl. Phys. **112**, 043512 (2012); doi: 10.1063/1.4747921
View online: http://dx.doi.org/10.1063/1.4747921
View Table of Contents: http://jap.aip.org/resource/1/JAPIAU/v112/i4
Published by the AIP Publishing LLC.

Tailoring the FeRh magnetostructural response with Au diffusion

M. Loving,[1] M. A. de Vries,[2,a)] F. Jimenez-Villacorta,[1] C. Le Graët,[2] X. Liu,[3] R. Fan,[4,b)] S. Langridge,[4] D. Heiman,[5] C. H. Marrows,[2] and L. H. Lewis[1]
[1]*Deparment of Chemical Engineering, Northeastern University, Boston, Massachusetts 02115, USA*
[2]*School of Physics and Astronomy, University of Leeds, Leeds LS2 9JT, United Kingdom*
[3]*National Synchrotron Light Source, Brookhaven National Laboratory, Upton, New York 11973, USA*
[4]*ISIS, Rutherford Appleton Laboratory, Harwell Science and Innovation Campus, Science and Technology Facilities Council, Oxon. OX11 0QX, United Kingdom*
[5]*Department of Physics, Northeastern University, Boston, Massachusetts 02115, USA*

(Received 25 April 2012; accepted 20 July 2012; published online 29 August 2012)

Factors which contribute to magnetostructural transition control have been demonstrated by study of the effects of Au incorporation on the magnetic and structural character of CsCl-structured equiatomic FeRh thin films. Sputtered films were capped with 2 nm of Au deposited at 873 K and at 323 K and subsequently characterized with magnetometry and synchrotron-based structural probes. Diffusion of Au into the FeRh film layer at 873 K is confirmed by a reduction in the Au capping layer thickness relative to the film capped at 323 K. The impact of Au diffusion on the FeRh magnetostructural character is noted by a decrease in the onset of the transition temperature, a thermally broadened first-order transition and an increased sensitivity of the transition to applied magnetic field. Additionally, magnetization data indicate that Au diffusion causes retention of the ferromagnetic phase well below the normal magnetostructural transition temperature. These results are attributed to a multiphase FeRh film layer created by thermally driven Au diffusion. [http://dx.doi.org/10.1063/1.4747921]

I. INTRODUCTION

Materials with coupled magnetic and structural phase changes—magnetostructural materials—have the potential to exhibit a large functional response to physical inputs such as small deviations in temperature, pressure, or magnetic field, and are thus of both basic scientific interest as well as technological interest for advanced sensor devices. The near-equiatomic phase of FeRh (denoted α'-FeRh), a model magnetostructural material with the chemically ordered CsCl (B2) structure, undergoes a first-order phase transition from antiferromagnetic (AF) to ferromagnetic (FM) character with a 10 K thermal hysteresis at approximately 370 K in bulk form, which is accompanied by a 1% volume expansion in the unit cell.[1–4] Numerous studies have shown that variations in the applied external magnetic field as well as strain can modify the magnetostructural phase transition character and transition temperature (henceforth denoted T_t) in both bulk and thin film forms of FeRh.[5–8] In particular, an applied magnetic field has been demonstrated to linearly decrease the transition temperature at a rate of -8 K/T in both bulk and thin film forms of FeRh.[5,9]

Thin film forms of FeRh are particularly interesting due to their heightened sensitivity to strain that may contribute to unique properties such as the observed persistence of retained ferromagnetism below the bulk phase transition temperature.[10–12] While the consequences of extrinsic physical parameter variation on α'-FeRh have been widely investigated, few reports to date have examined in detail the effects of chemical species lattice substitution on this transition, especially in thin film forms of FeRh.[13,14] In this work, information obtained from magnetic and synchrotron-based structural studies reveals that diffusion of Au into FeRh thin films with the CsCl structure leads to a magnetically, structurally, and compositionally graded layer of FeRh with an accompanying alteration of materials properties, including a reduction in the onset and abruptness of T_t. It is postulated that thermally driven diffusion in layered FeRh-based thin films can offer a means of tailoring the magnetostructural transition in this material to defined parameters and may lead to further advances and insight in the application of FeRh for future media and sensor applications.[15]

Over the past 40 years, several literature reports have indicated that the onset of the magnetostructural transition in strongly coupled materials, including FeRh, may be sensitively tuned by substitutional doping into the lattice. Modification of FeRh with noble metals (NMs) produces an alteration in the onset of T_t that is typically attributed to electronic effects;[16] however, typically little detail is furnished on the correlations between the structural and magnetic properties. Many NM lattice substitutions, such as Pt ($3 \leq$ at. $\% \leq 42.5$),[9,14,17–19] Ir ($1.5 \leq$ at. $\% \leq 7$),[9,17,19,20] Rh, and, Os (4.2 at. %),[17] are reported to produce an increase in T_t relative to the unmodified FeRh composition while maintaining a sharp AF-FM transition. Alternatively, alloying additions of Pd ($1.5 \leq$ at$\% \leq 13$)[9,16,17,20–24] and Au (at. $\% = 8.33$)[17] are found to decrease the onset of the magnetic phase transition T_t. Specifically, the transition temperature of bulk FeRh is reported to decrease from 350 K to 130 K with addition of 8.33 at. % Au and gives rise to a very large (40 K) thermal hysteresis, although the abruptness of this transition was not indicated. It is interesting to note that the magnetostructural

[a)]Present address: School of Chemistry, University of Edinburgh, Edinburgh EH9 3JJ, United Kingdom.
[b)]Present address: Diamond Light Source Ltd., Harwell Science and Innovation Campus, Oxon. OX11 0QX, United Kingdom.

properties of $(FeRh)_{1-x}Au_x$ compounds and alloys in general have not been subjected to deeper study as Au is a common capping layer for the protection of FeRh thin films from oxidation. In this work, the effects of thermally driven diffusion of Au into FeRh films are investigated to complement existing studies on this compound, with the primary conclusion that the introduction of Au into the FeRh lattice significantly alters the magnetostructural response by decreasing the onset and sensitivity of the transition. In this manner, elemental lattice substitution provides a potential route for tailoring the magnetostructural transition in FeRh.

II. EXPERIMENTAL DETAILS

Nominally, equiatomic FeRh thin films were grown by sputter deposition onto (001)-oriented MgO substrates. The films were deposited from separate Fe and Rh targets of 99.9% purity for 25 min at 873 K with an argon/2% H_2 sputter gas, at a growth rate of $\sim$0.04 nm/s with a base pressure of 3×10^{-7} Torr. A gold capping layer of approximately 2-nm thickness was deposited onto both films under two separate growth conditions. Under the first condition (denoted henceforth as "hot Au"), the Au layer was grown on the FeRh film surface directly after deposition at 873 K, maintained at this temperature for several hours and then annealed *in situ* at 973 K for 1.5 h leading to a 56.5 nm-thick film. In the second condition (denoted henceforth as "cold Au"), the FeRh film was annealed *in-situ* at 973 K for 1.5 h, then cooled down to 323 K prior to growth of the Au capping layer, leading to a film thickness of 49.2 nm. Under ideal conditions, attainment of very sharp interfaces between the film/substrate and film/cap would result in lattice mismatches between the FeRh/MgO and FeRh/Au interfaces of $+0.28\%$ and $+3.42\%$, respectively; these strains create a tetragonal FeRh lattice symmetry reduced from the perfect CsCl cubic symmetry. Both types of films appeared shiny after the deposition process, confirming the achievement of a metallic film. The equiatomic film composition was determined by energy dispersive x-ray spectroscopy with an accuracy of ± 3 at. %. The film layer thickness, interfacial width, and structure were assessed by x-ray scattering techniques. Specular and off-specular x-ray reflectivity (XRR) measurements were performed using a PANanalytical X'Pert PRO MPD Theta-2Theta Systems laboratory-based diffractometer. Interference (Kiessig) fringes were obtained with an in-plane scattering geometry; the periodicity of the Kiessig fringes indicates the film thickness, while the slope of the fringe envelope assesses the interfacial width of each layer. Here, the term interfacial width describes effects from both the compositional grading and diffuseness from interface roughness. As specular x-ray reflectivity measurements are only sensitive to the density difference in the direction normal to the sample surface and cannot explicitly distinguish between interfacial roughness and interdiffusion (i.e., a composition gradient), off-specular XRR data were collected at offsets from the specular reflection of 0.05° and 0.1°. The addition of off-specular x-ray reflectivity data provides complementary information to understanding the structural character of the films as it enables separation of contributions from the from interfacial roughness and compositional grading.

The specular XRR data were analyzed using a REFS MERCURY software package supplied by Bede scientific[25] to determine the thickness and interfacial width of the FeRh and Au layers. Thickness and interfacial width estimates of both films were made by fitting the specular XRR data with the simplest model to provide a reasonable fit to the experimental data. Thus, the fitting procedure utilized four distinct film layers in both the "hot Au" and "cold Au" films to model the architecture: equiatomic FeRh, Rh-rich FeRh, $(Fe_xRh_{1-x})_yAu_{1-y}$, and pure Au. Compositions for these layers were determined by setting a fixed composition of the equiatomic FeRh layer and then performing an optimization fitting of the XRR data. This procedure allowed more freedom in fitting the composition of the remaining film layers (i.e., the Rh-rich FeRh and the $(Fe_xRh_{1-x})_yAu_{1-y}$alloy). This model was found to produce a fit in excellent agreement with the experimental reflectivity data, as discussed in the following sections.

X-ray diffraction (XRD) experiments were conducted at the National Synchrotron Light Source Beamline X22C at Brookhaven National laboratory using a Franke & Heydrich 6-circle diffractometer with incident photon energy of 11 keV. Diffraction studies of the (002) FeRh Bragg peak in zero magnetic field were made as a function of temperature while traversing through the magnetostructural transition in the range of $300\,K \leq T \leq 424\,K$ with 10 K steps. The drift in temperature during data collection was ± 0.2 K. To ensure that no changes had occurred in the FeRh lattice during the thermal cycling, $(00L)$ XRD data were collected and compared before and after heating through the transition. The resultant Bragg peaks were indexed to a body-centered tetragonal (BCT) unit cell on the basis of the aforementioned lattice distortions at the film interfaces, fit with a double Pseudo-Voigt fitting function, and were compared to the reported bulk FeRh cubic lattice parameter of 0.2988 nm in the AF phase to get an estimate of film strain.[3,5]

Magnetic characterization of the films was carried out using a superconducting quantum interference device (SQUID) magnetometer (Quantum Design model MPMS–XL 5) in the temperature range $200\,K \leq T \leq 400\,K$ with a temperature sweep rate of 10 K/min and applied magnetic fields H up to 50 000 Oe. Magnetic moment (M) *vs.* temperature (T) data was collected with the field applied parallel to the film plane; no demagnetization corrections were applied. The magnetostructural phase transition temperature, denoted T_t, is defined as the inflection point of the M *vs.* T transition and is determined as the maximum of the derivative of M with respect to T (i.e., $\frac{\partial M}{\partial T}|_{max}$). The width of the thermal hysteresis of the FeRh magnetostructural transition is determined as the difference between the temperature midpoints of the M *vs.* T transition upon heating through the AF-FM transition and cooling through the FM-AF transition. The hysteretic (M vs. H) character of the films is assessed at 300 K.

III. RESULTS

Experimental results obtained from the FeRh films reveal a multifaceted view of the magnetostructural transition and confirm its sensitivity to capping layer character and

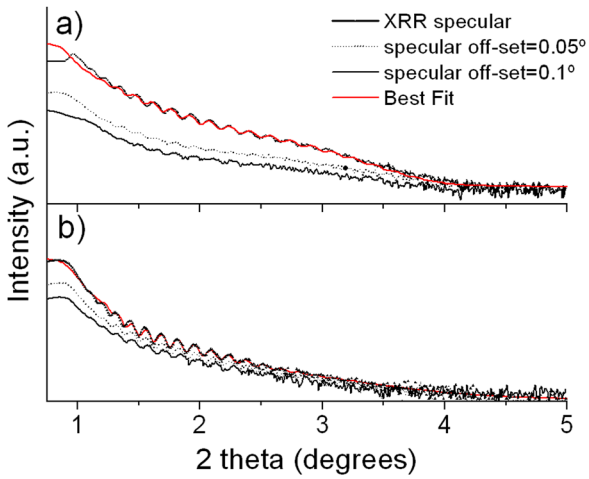

FIG. 1. Specular and off-specular x-ray reflectivity data for 50 nm-thick FeRh thin films with Au cap grown at (a) 323 K after FeRh film annealing at 873 K ("cold Au") and (b) Au cap grown at 873 K prior to FeRh annealing at 873 K ("hot Au"). The specular XRR fits, shown here, demonstrate goodness-of-fit values of ~0.1 indicating a good agreement between the calculated and measured curves.

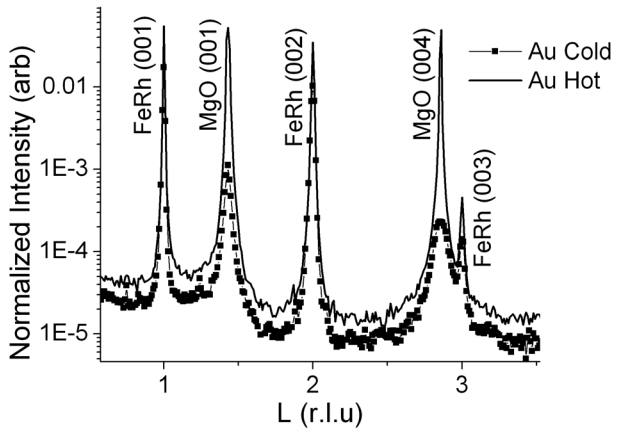

FIG. 2. (00*L*) x-ray diffraction patterns, given in reciprocal lattice units (*r.l.u*), for the "cold Au" (solid squares) and "hot Au" (solid line) FeRh thin films.

deposition conditions. In brief, a decrease in the Au capping layer thickness is accompanied by an increase in the interfacial width of the "hot Au" film as compared with the "cold Au" film. Differences in the thermal hysteresis behavior of the "hot Au" film relative to the "cold Au" film are observed as a reduction in the onset of the magnetostructural transition temperature T_t, a highly broadened thermo-magnetic transition occurring over a large temperature range, and an enhanced sensitivity of the magnetic transition to applied magnetic field. Furthermore, the "hot Au" film possesses significant retained ferromagnetism at room temperature and exhibits multiple phases of FeRh. These results are discussed in detail below.

A. Structural character of the films

The specular and off-specular x-ray reflectivity data, displayed in Figs. 1(a) and 1(b), qualitatively illustrate the differences between the individual film layer thickness and interfacial width values of the "hot Au" and "cold Au" films. Best fits to the specular XRR data, using the BEDE REFS software package, were obtained using bulk values for the MgO substrate density and under the assumption that all layers are fully dense. The individual film layer composition, thickness, and interfacial width values were varied to obtain best fits; the final results of these fits are listed in Table I for both the "hot Au" and "cold Au" films. The MgO substrate roughness values of both films were taken as 0.1 nm. The accuracy of the values displayed in Table I are not expected to exceed ±10% of the calculated compositional variation and 0.5 nm of the thickness and interfacial width values. Overall, the data shown in Table I indicate that while the calculated thicknesses of the equiatomic FeRh layer is similar for both the "hot Au" and "cold Au" films, the calculated thickness of the Au capping layer is reduced by almost a factor of three in the "hot Au" film. Inclusion of a $(Fe_xRh_{1-x})_yAu_{1-y}$ alloy layer and a Rh-rich FeRh layer in the BEDE REFS MERCURY software fit to the XRR data reveals an increased thickness of both of these layers in the "hot Au" film as compared with the "cold Au" film. Furthermore, each layer present in the "hot Au" film has a calculated surface interfacial width that is significantly greater than corresponding layers in the "cold Au" film. Most strikingly, the surface interfacial widths of the equiatomic FeRh and Au layers in the "hot Au" film are nearly three times greater than those of the "cold Au" film FeRh and Au layers.

The XRR data are complemented and deepened by synchrotron x-ray diffraction data collected on both samples, Figs. 2–4. The x-ray (00*L*) scans, Fig. 2, reveal a film-substrate orientation relationship of (001)-oriented FeRh on (001)-oriented MgO. As the (001) Bragg reflection is normally forbidden for body-centered crystal lattices, these results confirm attainment of the chemically ordered α'-FeRh phase during synthesis.[26] Differences observed in the MgO

TABLE I. Calculated composition, film thickness, and interfacial width values for both the "hot Au" and "cold Au" FeRh thin films based on the specular XRR fittings shown in Fig. 1; all thickness and interfacial width values are given in nm while compositions are listed in terms of at. %. Errors in the atomic compositions of the listed alloys are estimated at ±10% in the compositional variation and ± 0.5 nm in the thickness and surface interfacial width determinations.

	Calculated layer composition	$Fe_{0.24}Rh_{0.76}$	$Fe_{0.44}Rh_{0.56}$	$Fe_{0.01}Rh_{0.01}Au_{0.98}$	Au
"cold Au"	Thickness	0.2	45.2	0.4	3.5
	Interfacial width	0.8	0.7	0.7	0.7
	Calculated layer composition	$Fe_{0.20}Rh_{0.8}$	$Fe_{0.44}Rh_{0.56}$	$Fe_{0.04}Rh_{0.36}Au_{0.6}$	Au
"hot Au"	Thickness	3.3	48.6	4.5	1.4
	Interfacial width	1.0	2.2	1.4	2.2

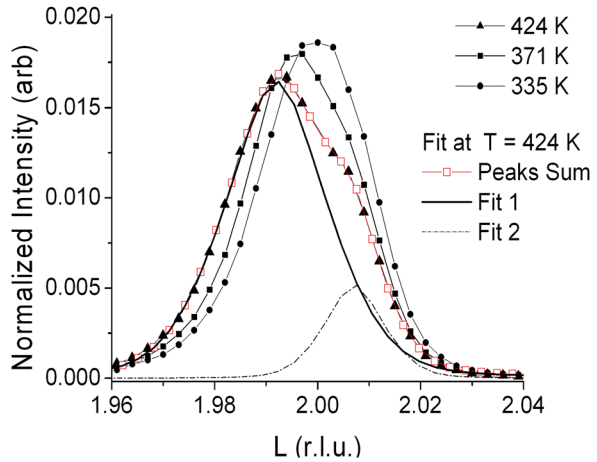

FIG. 3. (00*L*) x-ray diffraction patterns measured around the (002) Bragg reflection of the "hot Au" film at various temperatures during heating. The high temperature Bragg reflection at T = 424 K) corresponds to the FM phase and is fit with a double Pseudo-Voigt function. The "cold Au" (00*L*) XRD patterns are not shown here.

peaks of Fig. 2 are likely a result of substrate imperfections such as a slight tilt to the substrate surface.

The structural transition that accompanies the AF-FM magnetic transition is signaled by the shift of the (002) Bragg peak to lower *L*-values—i.e. to larger lattice parameters—with increasing temperature from 330 K to 424 K; this result is illustrated in Fig. 3 for the "hot Au" FeRh film. In contrast to the data collected from the "cold Au" sample, it is evident that the "hot Au" (002) Bragg diffraction peaks contain contributions from two disparate, but closely related, phases with out-of-plane lattice parameters that differ by 3%. The emergence of a secondary phase is signaled in the transition temperature region of $360\,\text{K} \leq T_t \leq 400\,\text{K}$ by the emergence of a shoulder in the (002) Bragg reflection at higher *L* values. These peaks were fit with a double Pseudo-Voigt function (as described in the Sec. II), shown in Fig. 3, to determine the out-of-plane lattice parameter values as a function of

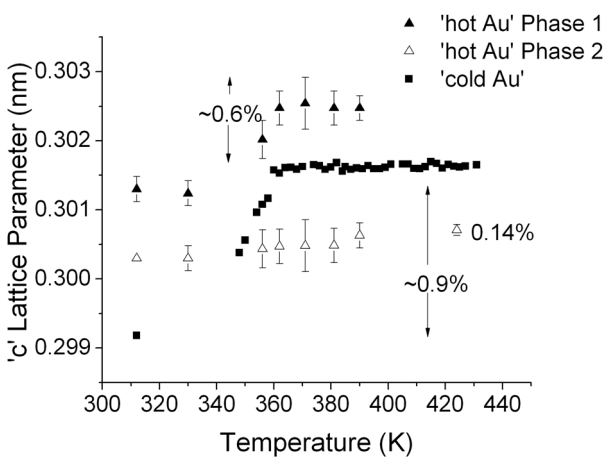

FIG. 4. Temperature dependence of the out-of-plane *c* lattice constant of Phase 1 (solid triangles) and Phase 2 (open triangles) in the "hot Au" FeRh film, upon heating to 424 K, and of the single phase in the "cold Au" (solid squares) FeRh film. The lattice parameter expansion of each phase in the "hot Au" film is found to be 0.14% and 0.6%, while the lattice parameter expansion of the phase in the "cold Au" film is ~0.9%. Phase 1 in the "hot Au" film is considered as the more equiatomic FeRh phase.

TABLE II. Lattice constants and strain parameters of the "hot Au" and "cold Au" FeRh thin films. The *c*-lattice parameter values were measured for BCT FeRh by x-ray diffraction at 300 K, in the AF phase. Note: *c*-parameters are listed for each of the independent phases in the "hot Au" film. Strain values are derived from the experimental lattice parameter for bulk FeRh in the AF phase (as described in the Sec. II).

	c-parameter BCT: phase 1	% strain	*c*-parameter BCT: phase 2	% strain
"hot Au" film	0.3012 ± (0.002) nm	+0.80	0.3002 ± (0.011) nm	+0.47
"cold Au" film	0.2992 ± (0.002) nm	+0.13		

temperature. The out-of-plane FeRh lattice parameters values at room temperature (300 K) of both the "hot Au" and "cold Au" films are summarized in Table II. Out-of-plane lattice parameters, calculated through the FeRh magnetostructural transition, show a 0.9% out-of-plane expansion of the "cold Au" film and reduced out-of-plane expansions 0.6% and 0.14% of the two phases of the "hot Au" film (Fig. 4).

B. Magnetic properties of the films

Consistent with literature reports, the FeRh films of this study exhibit an abrupt AF-FM phase transition upon heating with a thermal hysteresis that is typically of the order of 15 K.[5,9] However, the character of the magnetostructural transition differs between the two film types as illustrated by the thermal hysteresis curves measured in applied fields of 100, 20 000, and 50 000 Oe (Fig. 5). At $H = 100$ Oe, the onset of the transition with heating at $T_t = 360$ K in the "cold Au" film is abrupt and rather sharp, occurring over a 20 K temperature range while the transition of the "hot Au" film upon heating is suppressed by 30 K to 330 K and is much less abrupt, occurring over a wide range of temperature. Further, the magnitude of the thermal hysteresis of the transition in the "cold Au" film is smaller than that in the "hot Au" film at all applied fields, as seen in Fig. 5 and quantified in Fig. 6. Overall, the thermal hysteresis inherent in the "cold Au" film demonstrates a decreasing response to applied field (-1.2×10^{-4} K/Oe) while that of the "hot Au" film demonstrates an increasing response to applied field ($+1.2 \times 10^{-4}$ K/Oe). Both films exhibit saturation magnetization in the ferromagnetic regime (at ~400 K and $H = 100$ Oe) with a measured value of ~1250 emu/cm^3, which is in agreement with the reported saturation magnetization value of chemically ordered α'-FeRh (Fig. 5).[4] Table III summarizes features of the AF-FM and FM-AF transitions and the thermal hysteresis width, ΔT_t, of both films.

The multiphase character of the "hot Au" sample, first noted in the structural data (Sec. III A), may also be discerned by the temperature derivative of the magnetic moment at a given field (i.e., $\frac{\partial M}{\partial T}|_H$), Fig. 7, at higher temperatures (~360 K in applied magnetic fields >100 Oe, Fig. 7(d).) The width of the T_t transition of the "cold Au" film covers a 20 K span, 10 K smaller than that of the "hot Au" film, attesting to its more homogeneous nature. The

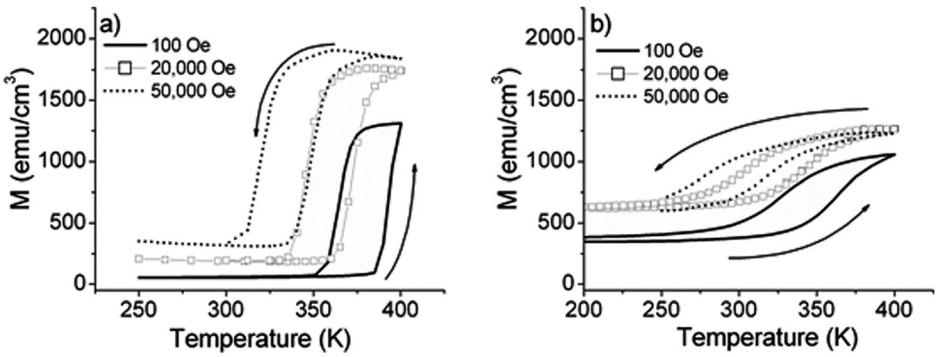

FIG. 5. Magnetization vs. temperature hysteresis loops, measured in a constant in-plane field, for (a) the "hot Au" and (b) the "cold Au" FeRh films.

sensitivity of the transition to applied magnetic field in both the AF-FM (heating) and FM-AF (cooling) transitions of the "hot Au" and "cold Au" films may be determined from Fig. 8. Here, the slope of the T_t *vs. H* plot, specifically dT_t/dH, of the "hot Au" film are -8.84×10^{-4} (+/− 0.01) K/Oe and -9.96×10^{-4} (+/− 0.01) K/Oe upon heating and cooling, respectively, while the "cold Au" film has values of -8.67×10^{-4} (+/− 0.02) K/Oe and -8.33×10^{-4} (+/− 0.02) K/Oe upon heating and cooling, respectively. The T_t value, upon heating, of the secondary phase in the "hot Au" film is difficult to discern; however, this secondary phase has a $\sim dT_t/dH$ of -3×10^{-4} K/Oe upon cooling.

Finally, it is noted that the field-dependent magnetization of the two samples in the low temperature regime (at 300 K), Fig. 9, are very different: the "hot Au" film has $M_s = 680$ emu/cm^3, $M_r = 485$ emu/cm^3, and $H_c = 300$ Oe, while the "cold Au" film has $M_s = 83$ emu/cm^3, $M_r = 43$ emu/cm^3, and $H_c = 50$ Oe. These data highlight differences in the metastable retention of the ferromagnetic phase of FeRh below the equilibrium magnetostructural transition temperature.

IV. DISCUSSION

The combination of structural and magnetic data collected from the Au-capped FeRh films subjected to the two separate growth conditions, "hot Au" and "cold Au" (as described in the Sec. II), are consistent with the occurrence of thermally driven diffusion of Au into the FeRh lattice of the "hot Au" FeRh film. The effect of Au diffusion on the FeRh magnetostructural transition is evidenced by both magnetic and structural data in the *M vs. T, M vs. H* plots, the XRR data, and the (00*L*) XRD patterns. These features are discussed in detail below.

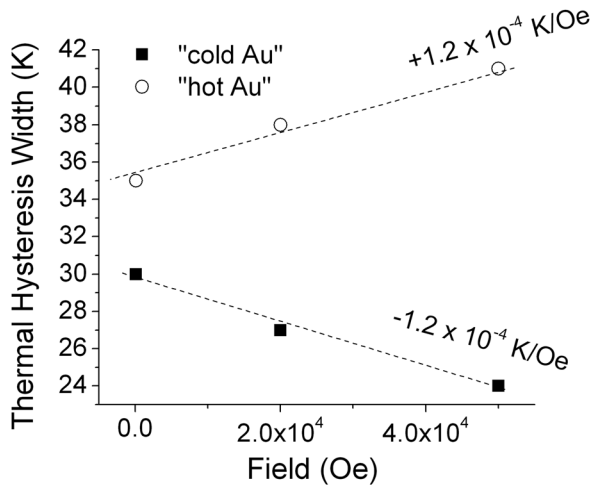

FIG. 6. Thermal hysteresis width as a function of applied magnetic field for the "hot Au" (open circles) and "cold Au" (closed squares) FeRh thin films.

Although both films of this study are highly chemically ordered, the XRR data indicate a larger interfacial width, a decreased Au layer thickness and an increased thickness of an $(Fe_xRh_{1-x})_yAu_{1-y}$ alloy layer in the "hot Au" film as compared with the "cold Au" film. As it was expected that equivalent amounts of Au were deposited on both samples during synthesis, these results indicate that nearly the entire Au capping layer has diffused into the FeRh film when deposited at high temperature. Furthermore, the results obtained from fitting the XRR data (Sec. III A) indicate that Au has substituted for Fe into the FeRh lattice, leading to the creation of a hypothesized pseudo-binary $(Fe_xRh_{1-x})_yAu_{1-y}$ layer and a subsequent Rh-rich FeRh layer at the FeRh/MgO interface. This conclusion is further validated by the fact that Fe and Au are nearly immiscible while Rh and Au are miscible.[27] The varied "hot Au" film architecture is anticipated to contribute to the multi-phase character of the magnetostructural transition observed in both the XRD and magnetic results. In particular, the secondary phase in the "hot Au" film (noted in Sec. III), identified as $(Fe_xRh_{1-x})_yAu_{1-y}$, possesses out-of-plane *c*-parameter at room temperature that is enhanced by 0.67% ("hot Au": $c = 0.3012$ nm; "cold Au": $c = 0.2992$) and coexists with the nominally pure binary α'-FeRh and Rh-rich FeRh phases. This enhanced *c*-parameter is analogous to *c*-parameter increases noted in Pd- and Pt-doped FeRh thin films: addition of 3 at. % Pd or Pt increases the room-temperature FeRh *c*-parameters to 0.3722 nm[23] (Pd-doped) and to $\sim$0.30 nm (Pt-doped).[14] Overall, the results presented here suggest that diffusion of Au into the FeRh film creates a compositionally graded layer of FeRh

TABLE III. Transition temperatures (T_t) and thermal hysteresis width (ΔT_t) of FeRh films as a function of applied field obtained from magnetization measurements.

Field (Oe)	"cold Au" heating (K)	"cold Au" cooling (K)	ΔT_t (K)	"hot Au" heating (K)	"hot Au" cooling (K)	ΔT_t(K)
100	394	364	30	362	327	35
20 000	372	345	27	342	304	38
50 000	348	324	24	318	277	41

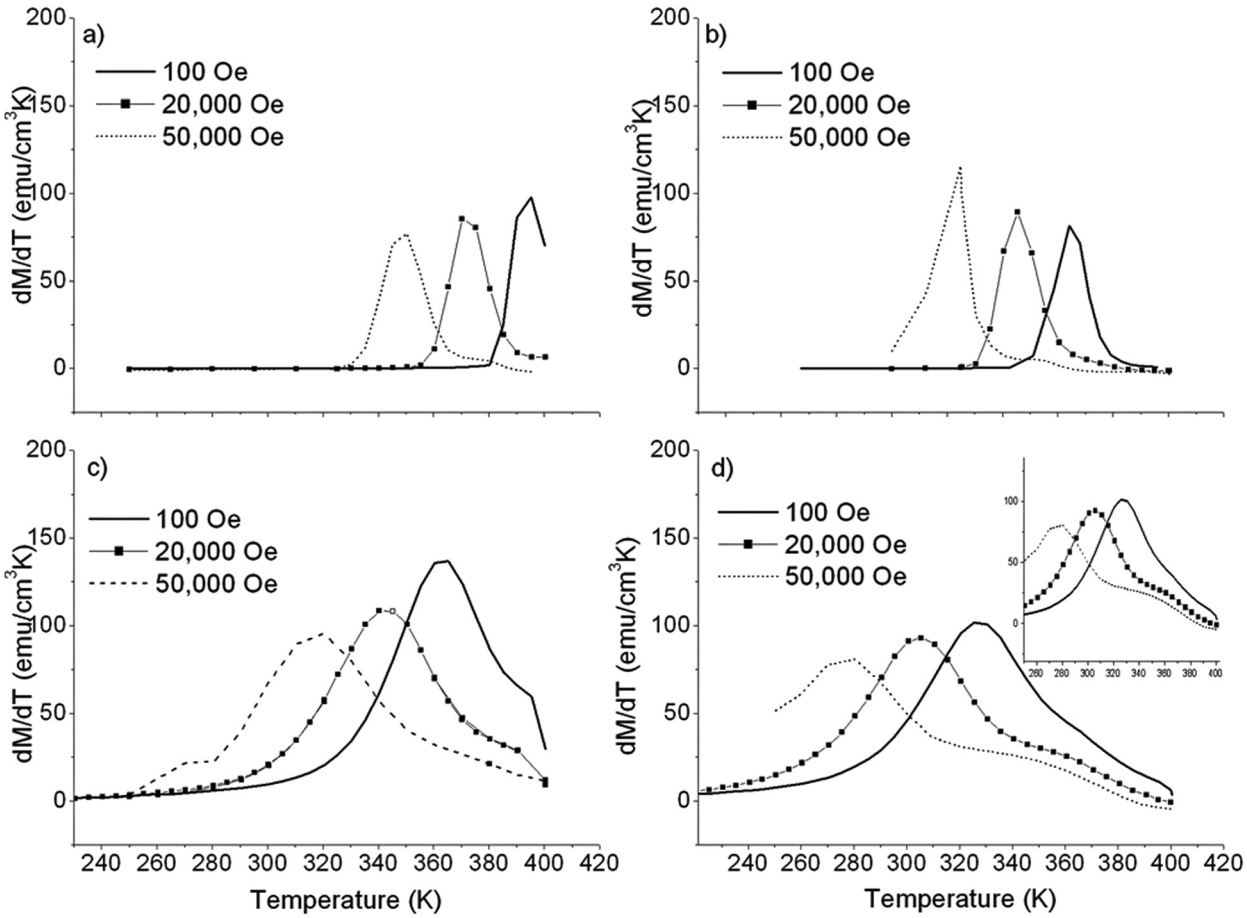

FIG. 7. Temperature derivative of magnetic moment for: the (a) heating branch and (b) cooling branch of "cold Au" FeRh film; and (c) heating and (d) cooling branches of the "hot Au" FeRh film. The inset of (d) shows a clear emergence of the secondary phase transforming upon cooling the temperature.

with multiple phases: chemically ordered α'-FeRh, Rh-rich FeRh, $(Fe_xRh_{1-x})_yAu_{1-y}$, and Au phases; this is shown schematically in Fig. 10. However, as previously noted, specular XRR alone cannot distinguish between roughness and interdiffusion (i.e., a composition gradient). The broad low bump in the specular XRR data of the "cold Au" film (located at 1.5°–3°) suggests that this film has a well-defined capping layer in comparison to that of the "hot Au" film. The off-specular XRR data serves as a complementary technique to separate interfacial roughness and compositional grading effects. The presence of Kiessig fringes in the off-specular XRR data collected on both samples indicates that there are similar well-defined layer structures at all lateral length scales and the differences in the samples are confined to the vertical profiles. This result qualitatively demonstrates that

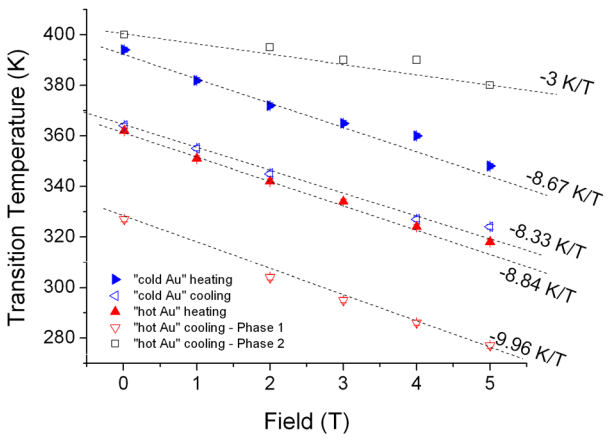

FIG. 8. Plot of the magnetostructural transition temperature, T_t as a function of applied magnetic field of the "hot Au" and "cold Au" FeRh thin films.

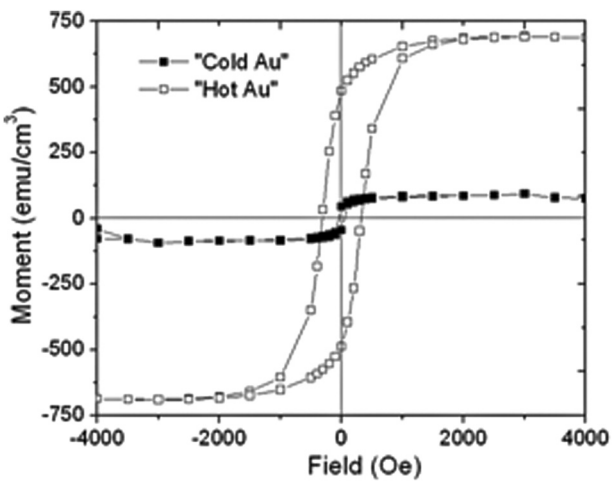

FIG. 9. M vs H plots measured at 300 K for both the "hot Au" (closed squares) and "cold Au" (open squares) indicating retention of considerable ferromagnetism at room temperature.

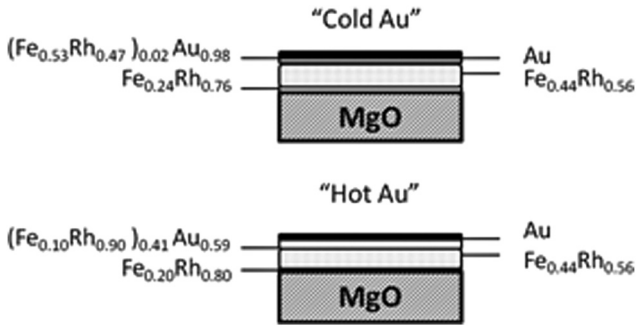

FIG. 10. Schematic of a simplified model of the "hot Au" and "cold Au" FeRh thin films of this study. The relative thicknesses and compositions listed in this schematic representation arise from the XRR data fitting results presented in Fig. 1.

there is indeed a greater degree of diffusion between layers in the "hot Au" film.

Both structural and magnetic data from the "hot Au" film demonstrate the inhomogeneous nature of the magnetostructural transition in this film. The asymmetry of the "hot Au" (00*L*) Bragg peaks confirms the existence of two distinct FeRh phases transitioning independently of one another. The FeRh out-of-plane lattice expansion accompanying the AF-FM transition in the "hot Au" film with increasing temperature is smaller by 50% than that of the "cold Au" film (Fig. 4). The 0.9% out-of-plane expansion of the "cold Au" film agrees with values observed for FeRh thin films of similar architecture; the two phases of the "hot Au" film demonstrate reduced *c*-parameter expansions of 0.6% and 0.14% (Fig. 4) relative to that of the "cold Au" film. The magnitude of this out-of-plane expansion is consistent with the 0.6% expansion reported for $FeRh_{0.95}Pt_{0.05}$ films grown on (001)-oriented MgO,[28] and likely reflects the $(Fe_xRh_{1-x})_yAu_{1-y}$ alloy formation in the FeRh layer.

The FeRh film character may be further assessed by the thermal hysteresis data that reveals the sensitivity of the film magnetostructural transition to applied magnetic field. In accordance with Landau-Devonshire theory, thermal hysteresis characterizes phase metastability associated with a first-order phase transition.[29] In this context, the increase in the magnitude of the thermal hysteresis with applied magnetic field (Fig. 6) noted for the "hot Au" film suggests that Au incorporation into the FeRh phase stabilizes the FM phase relative to equiatomic FeRh. The formation of the Rh-rich and $(Fe_xRh_{1-x})_yAu_{1-y}$ layers in the "hot Au" film are likely contributors to this effect as well as to the enhanced magnetic saturation value (M_s) of the *M vs. H* curve (Fig. 5) and likely underlies the increase in the nominally constant background moment observed in the *M vs. T* curve (Fig. 9).

Furthermore, the values of dT_t/dH (Fig. 8) measured in the "hot Au" film demonstrate an increase in the sensitivity of the transition to applied magnetic field upon both heating and cooling, relative to the "cold Au" film. Moreover, the observed sensitivity of the first-order transition of the secondary phase in the "hot Au" film upon cooling, to applied magnetic field ($dT_t/dH \sim -3 \times 10^{-4}$ K/Oe) agrees with the -3.3×10^{-4} K/Oe values reported for $Fe(Rh_{1-x}Pt_x)$ films,[14] this similarity with noble metal doping suggests that the secondary phase observed in the magnetic data in "hot Au" film may indeed be a result of the $(Fe_xRh_{1-x})_yAu_{1-y}$ phase formation.

The observed correlation between increased sensitivity of the phase transition temperature, T_t, and increased unit cell volume with Au incorporation in the FeRh film provides insight into the origins of the FeRh magnetostructural transition. In particular, a magnetovolume effect may be operative in conjunction with modifications to the electronic structure due to the addition of Au as the predominant mechanisms of the FeRh magnetostructural transition.

V. SUMMARY AND CONCLUSIONS

The magnetic and structural data obtained in this study provide fresh insight into the role of elemental substitution on magnetostructural transitions, particularly for FeRh thin films. The magnetic and structural data collected for samples subjected to different deposition protocols demonstrate that thermally driven Au can enter the FeRh lattice and alter the magnetostructural behavior. Films with thermally driven Au diffusion retain a CsCl-type order while also producing multiple phases of diverse structural and magnetic behavior. In particular, with the introduction of Au into the FeRh lattice, a reduced out-of-plane lattice expansion and increased out-of-plane lattice parameters are observed. Furthermore, with Au incorporation, the magnetic behavior demonstrates a more rounded transition occurring at lower temperatures and with a greater sensitivity of the inherent magnetostructural transition to applied field. The enhanced sensitivity of the FeRh magnetostructural transition, with Au diffusion, suggests that the origin of the transition may be linked to a magnetovolume effect. Thus, with Au diffusion, an increase in the thermodynamic driving force may cause the first-order magnetostructural transition to occur at lower temperatures and with greater sensitivity to applied magnetic field. Overall, these results may contribute to tailoring of the magnetostructural transition in FeRh films for future technological applications.

ACKNOWLEDGMENTS

Research was supported by the U.S. Department of Energy, Office of Basic Energy Sciences, Division of Materials Sciences and Engineering under No. DE-SC000525 [F.J.V.], by the National Science Foundation Grant No's. DMR-0908767 [M.L. and L.H.L.], DMR-0907007 [D.H.], and UK Engineering and Physical Sciences Research Council, Grant No. EP/G065640/1 [M.A.D., R.F., S.L. C.L., and C.H.M.]. Use of the National Synchrotron Light Source, Brookhaven National Laboratory, is supported by the U.S. Department of Energy, Office of Science, Office of Basic Energy Sciences, under Contract No. DE-AC02-98CH10886. Thank you to Alexandra Steele for efforts on the XRD peak fittings.

[1]M. Fallot, Ann. Phys. **10**, 291 (1938).
[2]M. Fallot and R. Hocart, Rev. Sci. **8**, 498 (1939).
[3]A. I. Zakharov, A. M. Kadomtseva, R. Z. Levitin, and E. G. Ponyatovskii, J. Exp.Theor. Phys. **46**, 2003 (1964).
[4]J. S. Kouvel and C. C. Hartelius, J. Appl. Phys. **33**, 1343 (1962).

[5]S. Maat, J. U. Thiele, and E. E. Fullerton, Phys. Rev. B **72**, 214432 (2005).
[6]J. van Driel, R. Coehoorn, G. J. Strijkers, E. Brück, and F. R. de Boer, J. Appl. Phys. **85**, 1026 (1999).
[7]Y. Ohtani and I. Hatakeyama, J. Magn. Magn. Mater. **131**, 339 (1994).
[8]L. I. Vinokurova, A. V. Vlasov, and M. Pardavi-Horvath, Phys. Status Solidi B **78**, 353 (1976).
[9]J. S. Kouvel, J. Appl. Phys. **37**, 1257 (1966).
[10]R. Fan, C. J. Kinane, T. R. Charlton, R. Dorner, M. Ali, M. A. de Vries, R. M. D. Brydson, C. H. Marrows, B. J. Hickey, D. A. Arena, B. K. Tanner, G. Nisbet, and S. Langridge, Phys Rev. B **82**, 184418 (2010).
[11]Y. Ding, D. A. Arena, J. Dvorak, M. Ali, C. J. Kinane, C. H. Marrows, B. J. Hickey, and L. H. Lewis, J. Appl. Phys. **103**, 07B515 (2008).
[12]J. M. Lommel, J. Appl. Phys. **40**, 1466 (1969).
[13]S. U. Jang, E. B. Park, J. H. Kim, K. H. Park, J. S. Lee, Y. K. Kim, S. Hyun, H. J. Lee, S. J. Kwon, and H. S. Lee, IEEE Trans. Magn. **46**, 2104 (2010).
[14]W. Lu, N. T. Nam, and T. Suzuki, IEEE Trans. Magn. **45**, 2716 (2009).
[15]J. U. Thiele, S. Maat, J. L. Robertson, and E. E. Fullerton, IEEE Trans. Magn. **40**, 2537 (2004).
[16]N. V. Baranov and E. A. Barabanova, J. Alloy Compd. **219**, 139 (1995).
[17]P. H. L. Walter, J. Appl. Phys. **35**, 938 (1964).
[18]P. A. Algarabel, M. R. Ibarra, C. Marquina, S. Yuasa, H. Miyajima, and Y. Otani, J. Appl. Phys. **79**, 4659 (1996).
[19]S. Yuasa, H. Miyajima, Y. Otani, K. Tsuji, Y. Katayama, K. Kusumi, H. Yokoyama, K. Yaoita, and O. Shimomura, J. Phys. Soc. Jpn. **63**, 855 (1994).
[20]P. Tu, A. J. Heeger, J. S. Kouvel, and J. B. Comly, J. Appl. Phys. **40**, 1368 (1969).
[21]R. C. Wayne, Phys. Rev. **170**, 523 (1968).
[22]M. R. Ibarra, P. A. Algarabel, C. Marquina, Y. Otani, S. Yuasa, and H. Miyajima, J. Magn. Magn. Mater. **140–144**, 231 (1995).
[23]P. Kushwaha, A. Lakhani, R. Rawat, and P. Chaddah, Phys. Rev. B **80**, 174413 (2009).
[24]P. Kushwaha, A. Lakhani, R. Rawat, and P. Chaddah, J. Phys.: Conf. Ser. **200**, 032038 (2010).
[25]M. Wormington, C. Panaccione, K. M. Matney, and D. K. Bowen, Philos. Trans. R. Soc. A London **357**, 2827 (1999).
[26]B. E. Warren, *X-Ray Diffraction*, edited by M. Cohen (Addison-Wesley, Massachusetts, 1969).
[27]T. B. Massalski, *Binary Alloy Phase Diagrams*, edited by H. Okamoto, P. R. Subramanian, and L. Kacprzak (ASM International, Materials Park, Ohio, 1990).
[28]W. Lu, B. Yan, and T. Suzuki, Scr. Mater. **61**, 851 (2009).
[29]A. F. Devonshire, Adv. Phys. **3**, 85 (1954).